Mechanism of Dihydrofolate Reductase Downregulation in Melanoma by 3-O-(3,4,5-Trimethoxybenzoyl)-(−)-Epicatechin

Luís Sánchez-del-Campo,[1] Soledad Chazarra,[1] María F. Montenegro,[1] Juan Cabezas-Herrera,[2] and José Neptuno Rodríguez-López[1*]

[1] *Department of Biochemistry and Molecular Biology A, School of Biology, University of Murcia, E-30100 Espinardo, Murcia, Spain*

[2] *Research Unit of Clinical Analysis Service, University Hospital Virgen de la Arrixaca, Murcia, Spain*

ABSTRACT

In our search to improve the stability and cellular absorption of tea polyphenols, we synthesized 3-O-(3,4,5-trimethoxybenzoyl)-(−)-epicatechin (TMECG), which showed high antiproliferative activity against melanoma. TMECG downregulates dihydrofolate reductase (DHFR) expression in melanoma cells and we detail the sequential mechanisms that result from this even. TMECG is specifically activated in melanoma cells to form a stable quinone methide (TMECG-QM). TMECG-QM has a dual action on these cells. First, it acts as a potent antifolate compound, disrupting folate metabolism and increasing intracellular oxidized folate coenzymes, such as dihydrofolate, which is a non-competitive inhibitor of dihydropterine reductase, an enzyme essential for tetrahydrobiopterin (H_4B) recycling. Such inhibition results in H_4B deficiency, endothelial nitric oxide synthase (eNOS) uncoupling and superoxide production. Second, TMECG-QM acts as an efficient superoxide scavenger and promotes intra-cellular H_2O_2 accumulation. Here, we present evidence that TMECG markedly reduces melanoma H_4B and NO bioavailability and that TMECG action is abolished by the eNOS inhibitor N_ω-nitro-L-arginine methyl ester or the H_2O_2 scavenger catalase, which strongly suggests H_2O_2-dependent DHFR downregulation. In addition, the data presented here indicate that the simultaneous targeting of important pathways for melanoma survival, such as the folate cycle, H_4B recycling, and the eNOS reaction, could represent an attractive strategy for fighting this malignant skin pathology. J. Cell. Biochem. 110: 1399–1409, 2010.   © 2010 Wiley-Liss, Inc.

KEY WORDS: MELANOMA; DIHYDROFOLATE REDUCTASE; CATECHINS; HYDROGEN PEROXIDE; GENE EXPRESSION

Dihydrofolate reductase (DHFR) is a necessary enzyme for maintaining intracellular pools of tetrahydrofolate (THF) and its derivatives, which are essential cofactors in one-carbon metabolism [Schweitzer et al., 1990]. Several studies have shown that protein and mRNA levels of DHFR are higher in tumor tissues and cancer cells than in their healthy counterparts and that high DHFR levels have been associated with poor clinical outcomes in such cancers [Nano et al., 2003; Sowers et al., 2003]. Tumors with elevated DHFR levels are thought to undergo more active cellular proliferation, which, in turn, is associated with tumor invasiveness and metastasis [Sowers et al., 2003]. Whether DHFR overexpression is a consequence of aberrant cellular proliferation or directly

stimulates the increase in cell growth and proliferation associated with the transformed phenotype remains unknown.

A connection between DHFR and tetrahydrobiopterin (H_4B) recycling has long been suspected, especially in neuronal and endothelial tissues. DHFR catalyzes the regeneration of H_4B from its oxidized form, dihydropterin (H_2B), in several cell types [Thony et al., 2000; Werner-Felmayer et al., 2002; Sugiyama et al., 2009], and it has recently been proposed that endothelial DHFR is critical for maintaining H_4B cellular levels and nitric oxide bioavailability [Chalupsky and Cai, 2005]. The data indicate that DHFR works in coordination with dihydropteridine reductase (QDPR), the main enzyme responsible for H_4B recycling [Thony et al., 2000]. In addition, folic acid and its derivatives are essential for reversing endothelial dysfunction via several putative mechanisms [Moat et al., 2004]. H_4B is an essential cofactor of a set of enzymes that are of central metabolic importance (i.e., the hydroxylases of the three aromatic amino acids, phenylalanine, tyrosine, and tryptophan, ether lipid oxidase, and the three nitric oxide synthase (NOS) isoenzymes). Due to the vital importance of H_4B recycling for the cells, we hypothesized that targeting this reaction could be an attractive strategy for cancer therapy, especially in melanoma. Melanoma cells require a continuous supply of H_4B to maintain melanin synthesis, the cofactor necessary to generate phenylalanine and tyrosine, which fuels the melanogenesis pathway.

Folic acid metabolism inhibitors, also called antifolates, are important agents for cancer chemotherapy [Schweitzer et al., 1990]; among them, methotrexate (MTX) is the most clinically used DHFR inhibitor. However, although DHFR is efficiently inhibited by MTX, DHFR gene amplification, which occurs in response to sustained exposure to this drug, is a commonly acquired resistance mechanism [Zhao and Goldman, 2003]. The resistance process involves an increase in the DHFR gene copy number, mRNA, and protein. Recently, we have shown that the ester-bonded gallate catechins isolated from green tea are potent inhibitors of DHFR activity in vitro [Navarro-Peran et al., 2005, 2007]. In our search to improve the stability and bioavailability of green tea polyphenols for cancer therapy, we synthesized a trimethoxy derivative of (−)-epicatechin-3-gallate (ECG), 3-O-(3,4,5-trimethoxybenzoyl)-(−)-epicatechin (TMECG), which showed high antiproliferative activity against malignant melanoma [Sánchez-del-Campo et al., 2008]. This compound is a pro-drug that is selectively activated by the specific melanocyte enzyme tyrosinase [Sánchez-del-Campo et al., 2009a]. Upon activation, TMECG generates a stable quinone methide that strongly and irreversibly inhibits DHFR. TMECG selectively disturbs folate transport and, important for this work, downregulates DHFR expression in SK-MEL-28 melanoma cells [Sánchez-del-Campo et al., 2009a]. Recently, we observed that this compound effectively suppressed the proliferation of melanoma cells in cultures by inducing apoptosis [Sánchez-del-Campo and Rodríguez-López, 2008]. TMECG treatment of melanoma cells resulted in the downregulation of antiapoptotic Bcl-2, the upregulation of proapoptotic Bax and the activation of caspase-3 [Sánchez-del-Campo and Rodríguez-López, 2008]. In the present work, we show how the connection between the DHFR-catalyzed pathway and H_4B recycling is important for controlling DHFR expression.

The present data suggest that TMECG might act as an efficient therapeutic drug against melanoma.

MATERIALS AND METHODS

MATERIALS

TMECG was synthesized from (−)-catechin (Sigma Chemical Co., Madrid, Spain) with the subsequent inversion of stereochemistry at carbon-3 [Sánchez-del-Campo et al., 2008] and by subsequent reaction with 3,4,5-trimethoxybenzoyl chloride (Sigma Chemical Co.). Mushroom tyrosinase (Sigma Chemical Co.) was used to synthesize its quinone methide-related product (TMECG-QM). QDPR from sheep liver, horseradish peroxidase (HRP) and catalase were purchased from Sigma Chemical Co. and used without further purification. DHF (90%) was obtained from Aldrich Chemical Co. (Madrid, Spain). NADH, MTX, H_4B, H_2B, and N_ω–nitro-L-arginine methyl ester (L-NAME) were purchased from Sigma Chemical Co. Reagent grade H_2O_2 (30% v/v) was obtained from BDH-Merck (Poole, UK) and its concentration was determined spectrophotometrically using $\varepsilon_{240\,nm} = 43.7\,M^{-1}\,cm^{-1}$. Antibodies for DHFR and QDPR were purchased from Sigma Chemical Co. and the Abnova Corporation (Taipei City, Taiwan), respectively.

CELL CULTURE EXPERIMENTS

Human melanoma SK-MEL-28 cells were obtained from American Type Culture Collection (ATCC, Manassas, VA). Cells were grown in modified Eagle's medium (MEM) containing 1 mM sodium pyruvate and 10% fetal bovine serum (FBS) under 5% CO_2/95% air atmosphere. Human epidermal melanocytes (HeM) were supplied by Gentaur (Brussels, Belgium) and were cultured in HAM-F10 medium supplemented with 10% FBS, antibiotics and human melanocyte growth supplement (Gentaur). For cell culture assay, the cells were plated in 75-cm^2 NUNC flasks and grown until they reached 70% confluence. Then cells were treated with vehicle, H_2O_2 (50–100 µM), and TMECG (20 µM), either alone or combined with L-NAME (0.5 mM). Some cells were pretreated with folate-catalase (200 units/ml) for 2 h before the addition of TMECG. Cell viability was evaluated using the MTT cell proliferation assay. Apoptosis induction was assessed by analysis of cytoplasmic histone-associated DNA fragmentation using a kit from Roche Diagnostics (Barcelona, Spain). Apoptosis is represented as the specific enrichment of mono- and oligonucleosomes released into the cytoplasm and was calculated by dividing the absorbance of treated samples by the absorbance of untreated controls.

MEASUREMENT OF QDPR ACTIVITY AND INHIBITION STUDIES

QDPR activity was measured at $25°C$, as described elsewhere [Firgaira et al., 1981], using the *quinonoid* form of 6,7-dimethyl-H_2-pterin (qDMPH$_2$; Sigma Chemical Co.). Because *quinonoid* pteridines are very unstable, they are continuously generated by the HRP-catalyzed oxidation of DMPH$_4$ in this assay. The standard reaction mixture contained 50 mM Tris–HCl (pH 7.2), 20 µg of HRP, 0.9 mM H_2O_2, 100 µM DMPH$_4$, 100 µM NADH, and 30 ng of QDPR, unless otherwise indicated. Experimentally, all components except DMPH$_4$ were incubated for 1 min prior to initiating the reaction by the addition of DMPH$_4$. NADH consumption was measured by

absorbance at 340 nm in a Perkin-Elmer Lambda-35 spectrophotometer. The initial rates were obtained from the rate of decrease of absorbance at 340 nm ($\varepsilon = 6{,}200\,M^{-1}\,cm^{-1}$). Inhibition studies were performed by incorporating 0.05–2 mM TMECG and TMECG-QM or 5–100 μM DHF into the reaction mixture described above. To reach high TMECG and TMECG-QM concentrations, these compounds were dissolved in dimethyl sulfoxide (Me$_2$SO); in the final assay, the Me$_2$SO concentration did not exceed 0.05%, a value that had no effect on QDPR activity (data not shown).

MEASUREMENT OF BIOPTERIN LEVELS IN MELANOMA CELL LYSATES

After treatment with the vehicle or 50 μM TMECG for 24 h, SK-MEL-28 monolayers were detached with trypsin/EDTA and resuspended in ice-cold PBS. Aliquots of $5{-}6 \times 10^6$ cells were centrifuged (500g, 10 min) and subjected to biopterin measurements [Bevers et al., 2006]. Briefly, cell pellets were lysed in cold extraction buffer [50 mM Tris–HCl, 1 mM DTT, and 1 mM EDTA (pH 7.4)]. The whole procedure was performed in the dark. Proteins were removed by the addition of 10 μl of a 1:1 mixture of 1.5 M HClO$_4$ and 2 M H$_3$PO$_4$ to 90 μl of extract, followed by centrifugation. Total biopterins (H$_4$B, H$_2$B, and biopterin) were determined by acid oxidation. For this experiment, 10 μl of 1% iodine in 2% KI solution was added to 90 μl of protein-free supernatant. H$_2$B and biopterin were determined by alkali oxidation by the addition of 10 μl of 1 M NaOH to 80 μl of extract followed by 10 μl of iodine/KI solution. Samples were incubated at room temperature for 1 h. Alkaline-oxidation samples were acidified with 20 μl of 1 M H$_3$PO$_4$. Iodine was reduced by the addition of 5 μl of fresh ascorbic acid (20 mg/ml). Fifty microliters of supernatant was then injected into an HPLC system (Hitachi, LaChrom Elite) equipped with a 250 mm × 4.6 mm C18 column and a highly sensitive fluorescent detector (Schimadzu model RF-10Axl). The mobile phase was 5% methanol running at 1 ml/min. Excitation and emission wavelengths of 350 and 450 nm were used to detect fluorescent H$_4$B and its oxidized products. The absolute contents of H$_4$B and H$_2$B were calculated against a standard curve prepared with purified H$_4$B and H$_2$B that went through identical extraction procedures and is presented as picomoles per 10^6 cells.

OVEREXPRESSION OF QDPR IN SK–MEL–28 MELANOMA CELLS

QDPR expression vector (pCMV-QDPR) was purchased from Origene Company (Rockville). Transfections were conducted by Lipofectamine method. Briefly, for transient transfection, SK-MEL-28 cells were seeded in 6-well plates at a density of 4×10^5 cells/well. The following day, cells were transfected with 4 μg of QDPR expression vector or pcDNA3 (negative control) using Lipofectamine 2000 (Invitrogen, Barcelona, Spain). Following transfection, cells were maintained in appropriate medium and treated with vehicle or TMECG.

MEASUREMENT OF eNOS ACTIVITY IN INTACT CELLS

Endothelial nitric oxide synthase (eNOS) activity was determined using a fluorimetric NOS detection system (Sigma Chemical Co.) according to the manufacturer's protocol. The kit measures the intracellular production of NO using a cell-permeable diacetate derivative of 4,5-diamino-fluorescein (DAF-2-DA) [Kojima et al., 1998]. DAF-2-DA rapidly penetrates cells, where it is hydrolyzed by intracellular esterase activity to DAF-2, which reacts in turn with the NO produced by NOS to form a fluorescent triazolofluorescein. SK-MEL-28 cells were grown to 90% confluence in a black bottom 96-well plate and treated with vehicle or 50 μM TMECG for 24 h. Cells were washed and incubated with 5 μM DAF-2-DA for 1 h at room temperature in the dark. After incubation, cells were washed twice and incubated with arginine substrate solution and the appropriate reaction buffer supplied in the kit; fluorescence was then measured at the specified times (excitation and emission wavelengths at 485 and 530 nm, respectively; Fluostar Galaxy, BMG-Labtechnologies).

NBT ASSAY

The method chosen to assay the superoxide-scavenging properties of TMECG and TMECG-QM was a modification of an indirect inhibition assay developed to determine superoxide dismutase activity [Spitz and Oberley, 1989]. Xanthine–xanthine oxidase was used to generate a superoxide flux. NBT reduction by superoxide to blue formazan was followed at 560 nm in a Perkin-Elmer Lambda-35 spectrophotometer at room temperature. When increasing concentrations of TMECG or TMECG-QM were added to the system, the rate of NBT reduction was gradually inhibited. The amount of inhibition was defined as the percentage of the reference rate of NBT reduction in the absence of these compounds. The assay mixture also contained catalase to remove H$_2$O$_2$ and EDTA to chelate metal ions capable of redox recycling and interfering with the assay system. Each 1-ml assay tube contained the final concentrations of the following reagents: 50 mM sodium phosphate buffer (pH 7.4), 1 mM EDTA, 1 unit catalase, 60 μmol/L NBT, 0.1 mM xanthine, and 0.05 units xanthine oxidase.

WESTERN BLOT ANALYSIS

For immunoblot analysis, 25–50 μg of protein was subjected to SDS–PAGE and transferred to nitrocellulose membranes. Membranes were incubated for 1 h in blocking solution (Tris-buffered saline containing 1% Tween-20 and 5% non-fat dry milk) and further incubated overnight at 4°C with DHFR (1:250) and QDPR (1:150) antibodies. The membranes were then washed with blocking solution and incubated for 2 h with anti-mouse or anti-rabbit secondary antibodies conjugated with HRP. Bound antibodies were detected by chemiluminiscence (ECL Plus detection kit; GE Healthcare Life Sciences, Barcelona, Spain).

RNA ISOLATION AND RT–PCR

SK-MEL-28 and HeM polyA$^+$ mRNA was extracted from 5×10^6 cells using the Illustra Quick Prep Micro mRNA purification kit (GE Healthcare Life Sciences). mRNA (200 ng) was used to synthesize cDNA using the SuperScript First-Strand Synthesis System (Invitrogen). PCR amplification of 2 μl of the generated cDNA strand was carried out in a total volume of 50 μl using an Eppendorf Mastercycler thermal cycler. Samples were amplified by 40 cycles at 95°C (1 min), 62°C (1 min), and 72°C (1 min). The amplified PCR products were subjected to electrophoresis in 3% agarose gels and stained with ethidium bromide.

QUANTITATIVE REAL–TIME PCR ANALYSIS

cDNA samples (0.1 μl) were used for real-time PCR in a total volume of 20 μl using SYBR Green Reagent (Applied Biosystems, Foster City, CA) and specific primers on a 7500 Real Time PCR System from Applied Biosystems. The PCR amplification cycles included both denaturation (95°C; 15 min) to activate HotStart Taq DNA polymerase and minimize primer–dimer contribution and amplification [over 40–50 cycles including denaturation (94°C; 30 s), annealing (55°C; 30 s), and extension (72°C; 1 min)]. All PCR reactions were performed in triplicate and from at least two independent experiments. A non-RT control and negative control samples (without template) were processed in the same manner. Amplification specificity was verified by melting curve analysis for all samples and occasionally by agarose gel electrophoresis. Amplification of the target gene sequences were compared against serial dilutions of known quantities of their purified cDNA fragments and normalized to the abundance of the house-keeping gene β-actin.

PRIMERS FOR PCR

Primers were designed using Primer Express version 2.0 software (Applied Biosystems) and synthesized by Invitrogen. The primer sequences are as follows: DHFR (forward: 5′-ATG CCT AAA AAC TTA CTG AAC AAC CA-3′; reverse: 5′-TGG GTG ATT CAT GGC TTC CT-3′); QDPR (forward: 5′-AAG GGT TCG ATT CGG AGC TG-3′; reverse: 5′-TGC ATC CAC CTT CTC TTC AC-3′); and eNOS (forward: 5′-GAC GCT ACG AGG AGT GGA AG-3′; reverse: 5′-GAG TAG TAC CGG GGC TGG AG-3′); β-actin (forward: 5′-AGA AAA TCT GGC ACC ACA CC-3′; reverse: 5′-GGG GTG TTG AAG GTC TCA AA-3′). QDPR overexpression was confirmed by real-time and conventional PCR using the primers 5′-AGG TGA CTG CTG AGG TTG GA-3′ (forward) and 5′-GGA GCA CAG CGA TGG CGG CT-3′ (reverse).

FOLATE CONJUGATION WITH CATALASE

Folic acid was conjugated with catalase using the method described by Lee and Murthy [2007]. The activity of folate-conjugated catalase was determined by measuring the decomposition rate of H_2O_2.

STATISTICAL ANALYSIS

Data are presented as the mean $\pm$ SD from five to 10 independent experiments. Differences in biopterin and NO levels between control and TMECG-treated SK-MEL-28 melanoma cells were compared using a paired Student's t-test. Likewise, mRNA and proteins levels of DHFR, QDPR and eNOS in cells treated with TMECG alone or combined with L-NAME or catalase were compared with controls using Student's t-test. Statistical significance was set for $P < 0.05$.

RESULTS

TMECG EFFECTIVELY DOWNREGULATED DHFR AND QDPR IN HUMAN MELANOMA CELLS

Recently, we had reported that an intracellular activated product of TMECG, TMECG-QM, irreversibly inhibited human DHFR with an inhibition constant (K_i) of 8.2 nM [Sánchez-del-Campo et al., 2009a]. In addition to DHFR inhibition, TMECG treatment also modulated DHFR expression (Fig. 1A). The levels of DHFR mRNA were significantly higher in SK-MEL-28 melanoma cells than in normal melanocytes (estimated as 400- to 500-fold higher). Treatment of SK-MEL-28 cells with 20 μM TMECG for 3 days decreased the DHFR mRNA to levels similar to those detected in normal melanocytes (Fig. 1A). Protein levels showed good correlation with gene expression (Fig. 1A). Because DHFR has been implicated in H_4B recycling [Chalupsky and Cai, 2005] and to understand the mechanism of DHFR downregulation by TMECG, we decided to study the effect of this compound on the main H_4B recycling enzyme, QDPR. Although TMECG and its activated metabolite, TMECG-QM, did not inhibit QDPR over a millimolar range of concentrations (Fig. 1B), treating SK-MEL-28 cells with TMECG affected QDPR expression (Fig. 1C). Fig. 1C, illustrates that QDPR was overexpressed in SK-MEL-28 cells compared with normal melanocytes, with the increase estimated at approximately tenfold. Treatment of SK-MEL-28 cells with 20 μM TMECG for 3 days decreased QDPR mRNA levels 2.6-fold, bringing the levels closer to that of normal melanocytes (Fig. 1C). Similar patterns were observed when the protein levels were examined by Western blot analysis (Fig. 1C).

DHF IS A NON–COMPETITIVE INHIBITOR OF QDPR

The observed inhibition of DHFR by the active TMECG intermediate formed in melanoma cells suggested that its antifolate activity could trigger the constellation of events observed in cells after TMECG treatment. The inhibition of DHFR has profound effects on cellular metabolism, depleting the pool of THF coenzymes and accumulating the enzyme reaction substrate, DHF. An excess of DHF has been described as an important factor in antifolate cytotoxicity because it efficiently inhibits folate cycle enzymes, such as methyltetrahydrofolate reductase (MTHFR) [Lucock and Roach, 2005]. Therefore, the inhibition of QDPR by DHF was investigated, and the results indicated that DHF does indeed inhibit QDPR activity (Fig. 2A). Plots of the initial steady-state rate (v_0) versus the pteridine enzyme substrate in the absence and presence of different DHF concentrations indicated that the inhibitor modified the V_{max} of the reaction, but not the K_m of the enzyme, which was calculated to be 36.8 ± 5.0 μM. This behavior is typical of non-competitive inhibition, and Dixon plots of the reciprocal of v_0 versus (DHF) in the presence of different qDMPH$_2$ concentrations yielded a K_i of 16.3 ± 2.0 μM (Fig. 2B), which is even lower than the calculated K_m value for qDMPH$_2$. The data indicated that DHF can be a potent inhibitor of QDPR in vivo after intracellular accumulation and that this inhibition could result in H_4B oxidative inactivation in the presence of TMECG.

TMECG DEPLETES INTRACELLULAR H_4B IN MELANOMA CELLS

QDPR inhibition is anticipated to blunt H_4B recycling. The determination of total biopterin after acid oxidation extraction pointed to low levels of these compounds in SK-MEL-28 cells (Fig. 3A), whereas TMECG treatment produced a significant increase in the content of total biopterin (Fig. 3A). Assays performed to detect the H_4B and H_2B content separately, following basic oxidation of the extract, revealed very low levels of H_4B in TMECG-treated and untreated cells, confirming that almost all of the biopterin content was H_2B (Fig. 3A). First, we believe that the non-detection

of H_4B could be related to the oxidant nature of melanoma extracts. Melanoma cells are rich in oxidant compounds and the reactions of H_4B with ROS and/or quinonic compounds derived from the melanogenesis pathway are well established [Vasquez-Vivar et al.,

Fig. 1. Effect of TMECG (20 μM) on DHFR (A) and QDPR (C) expression in SK–MEL–28 melanoma cells after 3 days of treatment. Left panels represent the semiquantitative determination of DHFR and QDPR mRNA by real–time PCR. Histogram bars represent the number of copies of mRNA per 1×10^6 copies of β–actin obtained from ten PCR determinations in four independent experiments $\pm$ SD. $^*P < 0.05$ when comparing treated cells with control experiments. Images represent RT–PCR analysis for DHFR and QDPR compared with β–actin. Right panels show Western blot analysis for DHFR and QDPR in the studied cellular systems. Bars represent the differences in protein levels obtained from densitometric data from six independent analyses $\pm$ SD. $^*P < 0.05$ when comparing treated cells with control experiments. B: Effect of TMECG and TMECG–QM on QDPR activity.

2001; Garcia-Molina et al., 2007]. Therefore, it was likely that in this oxidative environment H_4B evolved into another species, which was not properly resolved in our HPLC analysis. In an attempt to overcome this problem, we determined the H_4B in melanoma extracts without the melanosome fraction, which is rich in oxidant compounds. However, the results were similar to those obtained with overall extracts (data not shown). The results were then interpreted assuming that the total biopterin content is very low in melanoma cells. In melanoma cells, H_4B is a coenzyme involved in multiple enzyme reactions, among them tyrosine and L-dopa synthesis and the NOS reactions. All these processes depend on a continuous supply of H_4B through "de novo" synthesis and regeneration pathways [Thony et al., 2000]; therefore, the steady-state concentration of both H_2B and H_4B must be very low in melanoma cells. Blockage of the recycling step by TMECG is believed to generate a dead-end pathway with the subsequent accumulation of H_2B. To check this hypothesis we studied the cellular response of SK-MEL-28 melanoma cells to TMECG after QDPR overexpression (Fig. 3B). The data indicated that the growth of cells overexpressing QDPR was scarcely inhibited by TMECG, being these transfected cells highly resistant to TMECG-induced apoptosis (Fig. 3B). All together, the results indicated that blockage of the H_4B recycling in SK-MEL-28 melanoma cells by TMECG is essential for its cytotoxic action.

TMECG INDUCES eNOS UNCOUPLING

Recent studies have demonstrated that H_4B deficiency may cause the "uncoupling" of eNOS. Under physiological conditions, H_4B binds to eNOS, resulting in the production of NO and L-citrulline from L-arginine and O_2, whereas eNOS produces superoxide anions in its "uncoupled" state. The involvement of eNOS on the effects of TMECG was demonstrated by several experimental approaches. eNOS is constitutively expressed and its expression has recently been detected in human malignant melanoma [Tu et al., 2006]. For this reason, the content of eNOS mRNA in control SK-MEL-28 melanoma cells and in cells subjected to TMECG treatment was measured by real-time PCR analysis; the DHFR/eNOS and QDPR/eNOS ratios are presented in Figure 4A. TMECG treatment significantly decreased the DHFR/eNOS and QDPR/eNOS ratios with respect to untreated cells, implying that substantially less DHFR and QDPR per se is available to supply recycled H_4B to eNOS. Next, a standard fluorimetric method was used to assay the eNOS activity in control and treated cells. Cells were loaded with the eNOS substrate,
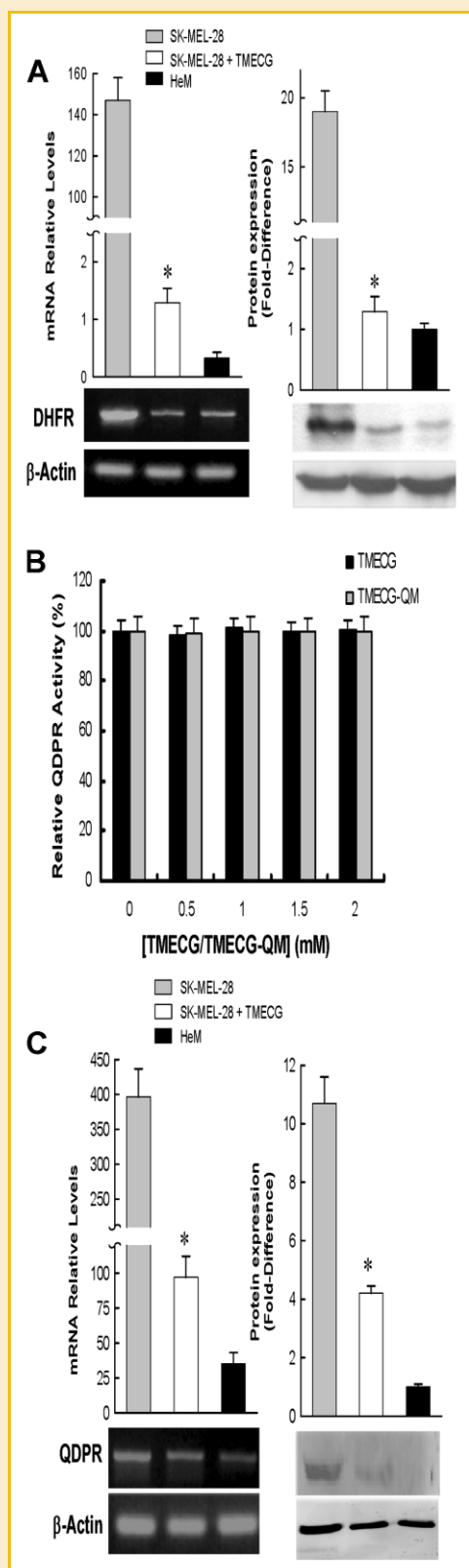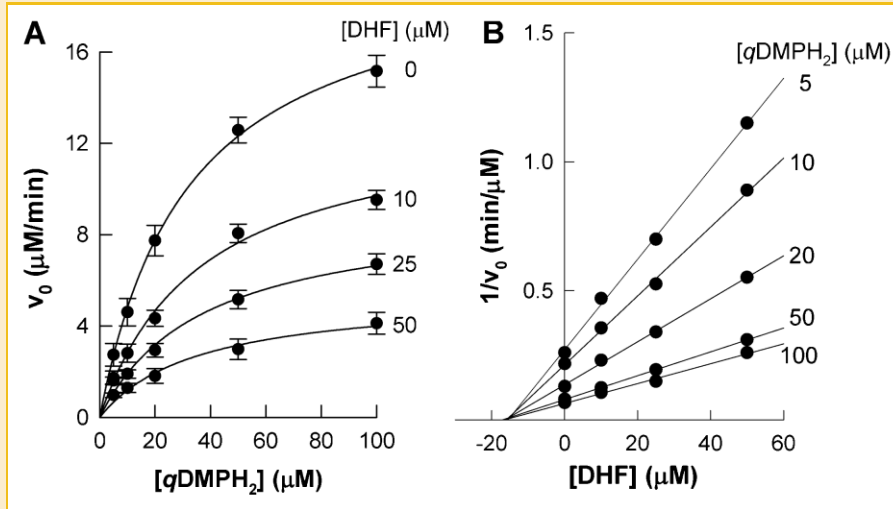
Fig. 2. Inhibition studies of QDPR by DHF. A: Plots of the initial steady-state rate (v_0) versus different concentrations of the pteridine enzyme substrate in the absence or presence of different DHF concentrations. Data points represent the means of ten activity determinations $\pm$ SD. B: Dixon plots of the reciprocal of the v_0 versus (DHF) in the presence of different qDMPH$_2$ concentrations.
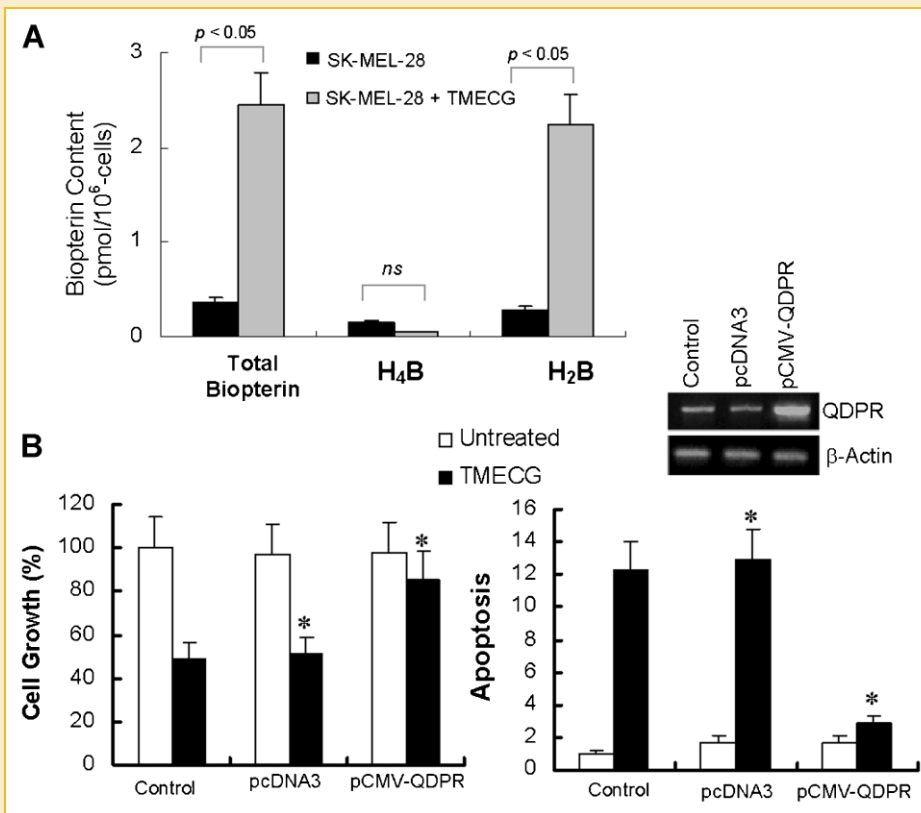

Fig. 3. Effect of TMECG on SK-MEL-28 biopterin levels and effect of QDPR overexpression on TMECG cytotoxicity. A: Determination of biopterin level in melanoma cell lysates subject to 24-h treatments with vehicle or TMECG (50 μM). Bars represent the mean of five different HPLC determinations in three independent experiments $\pm$ SD; ns, non-significant differences. B: Cell growth and apoptosis of SK-MEL-28 after 3 days of 50 μM TMECG treatment. Data are presented as the mean $\pm$ SD of three independent experiments. Cell growth and apoptosis data were expressed assuming 100% of growth and 1 of apoptosis for untreated controls. *Differences in cellular response to TMECG between cells transfected with pcDNA3 (negative control) and pCMV-QDPR were statistically significant ($P < 0.05$). A RT-PCR analysis of mRNAs extracted from those cells using specific primers for QDPR and β-actin is shown.
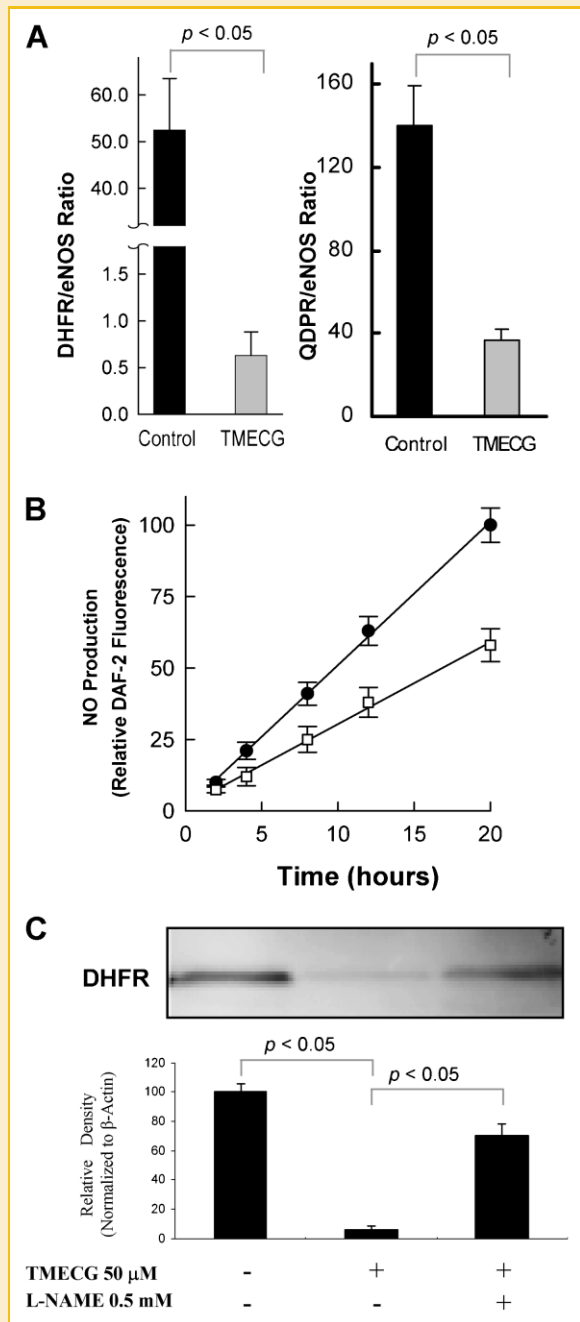
Fig. 4. Effect of TMECG on eNOS reaction. A: Grouped data on DHFR/eNOS and QDPR/eNOS mRNA ratios (n = 5). mRNA levels were determined by real–time PCR and the data are presented as the mean ± SD. Expression levels were normalized to the abundance of β–actin. B: Time–dependent NO production in SK-MEL-28 cells treated with vehicle (●) or 50 μM TMECG (□). Data are presented as the mean (n = 5) ± SD. Differences between groups at 20 h were statistically significant ($P < 0.05$). C: Western blot analysis of the effect of L–NAME on the TMECG–induced downregulation of DHFR after 3 days of treatment. The data shown are from a representative experiment repeated three times with similar results.

L-arginine and an appropriate fluorescent probe to detect NO (DAF-2). As observed in Figure 4B, TMECG inhibited NO production in melanoma cells. The effects of L-NAME, a selective inhibitor of eNOS, on TMECG-induced DHFR downregulation were also

analyzed (Fig. 4C). The presence of L-NAME in the culture medium reversed the effects of TMECG, highlighting the importance of eNOS in TMECG action. Therefore, the data indicated that although TMECG diminished NO formation, it did not inhibit eNOS in vivo. Taken together, the results suggested that the eNOS "uncoupled" reaction is the predominant pathway in the presence of TMECG, leading to the inhibition of NO production. Thus, the presence of TMECG switches the coupled eNOS reaction to an uncoupled reaction as a result of the failed H_4B recycling.

H_2O_2 IS REQUIRED FOR TMECG–INDUCED DOWNREGULATION OF DHFR AND QDPR

The idea that superoxide is a potent cell-damaging agent has long been controversial because this anion is considered poorly reactive [Benov, 2001]. The superoxide may cause cell damage, not directly but by participating in the so-called iron-mediated Haber-Weiss reactions to generate the highly reactive hydroxyl radical [Halliwell, 1978]. The presence of superoxide scavengers, such as superoxide dismutase or antioxidant compounds, quickly produces the dismutation of this reactive oxygen species to generate H_2O_2. Therefore, our next step was to examine the superoxide-scavenging properties of TMECG-QM, the major species in melanoma after TMECG treatment. Under most of the conditions tested, TMECG-QM was a very stable species; for example, it was stable for more than two months and suffered no apparent transformation in O_2-containing buffers. TMECG-QM did not react with H_2O_2, H_4B, ascorbic acid, NADPH or the oxidized or reduced forms of glutathione. However, TMECG-QM was very reactive in the presence of xanthine oxidase-generated superoxide, indicating the high superoxide scavenging capacity of this compound (Fig. 5A). The results suggested that the superoxide generated by eNOS uncoupling can rapidly generate H_2O_2 in the presence of TMECG-QM. This finding is of importance because H_2O_2 directly produced by or derived from superoxide has emerged as a possible signaling intermediate in several types of cells, where it mediates a variety of gene regulatory responses [Cai et al., 2003; Hasse et al., 2004; Cai, 2005]. Interestingly, H_2O_2 has been proposed to mediate DHFR and QDPR activity and expression in endothelial and human epidermal cells, respectively [Hasse et al., 2004; Chalupsky and Cai, 2005; Sugiyama et al., 2009]. Whether TMECG would induce the downregulation of DHFR through the intracellular formation of H_2O_2 was investigated in our laboratory using two independent approaches. The first approach was to examine the effect of exogenously applied H_2O_2 on the expression of this enzyme in SK-MEL-28 cells. As observed in proliferating endothelial cells [Chalupsky and Cai, 2005], H_2O_2 (at 100 μM) downregulated melanoma DHFR expression, which resulted in lower protein levels (Fig. 5B). The second approach involved the studying the effect of the addition of a scavenger of intracellular H_2O_2 to SK-MEL-28 cells treated with TMECG. Thus, we designed strategies to deliver catalase into SK-MEL-28 cells. A method that exploits folate receptor α (FRα) endocytosis has been successfully employed to deliver active proteins into living cells [Lee and Murthy, 2007]. As SK-MEL-28 cells constitutively express the FRα [Sánchez-del-Campo et al., 2009b], folate was conjugated to catalase and the complex folate-catalase was used to deliver the enzyme into SK-MEL-28 cells.
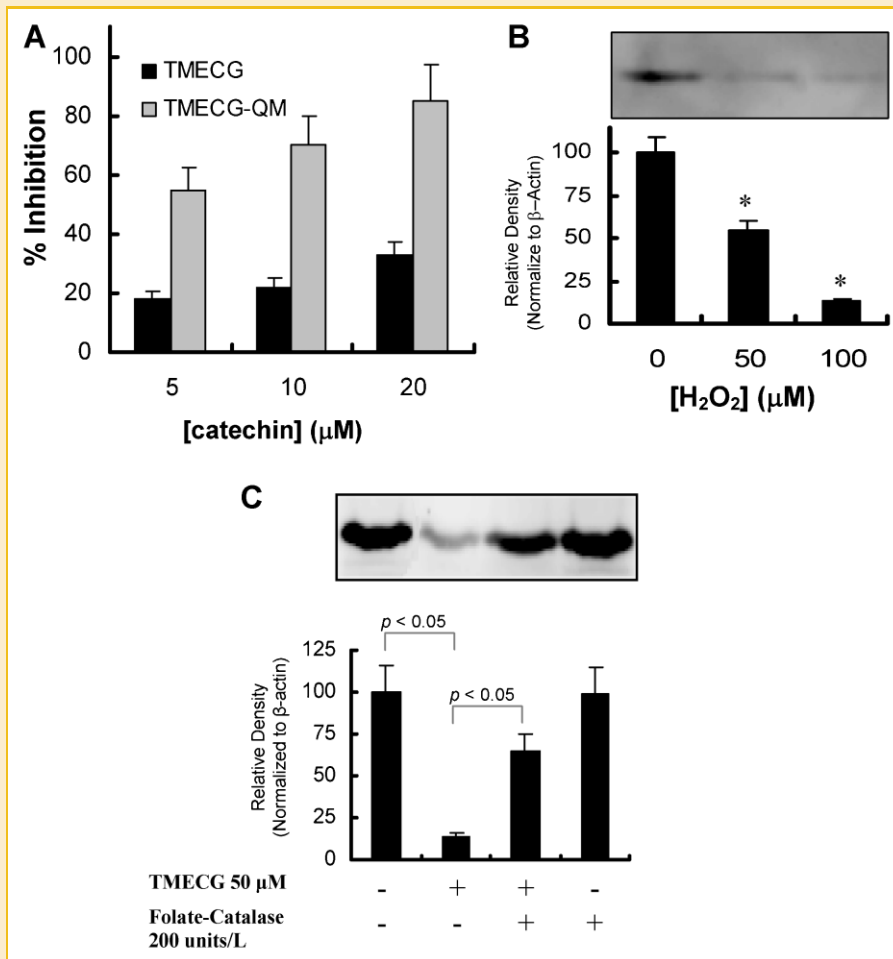
Fig. 5. Superoxide scavenging properties of TMECG and TMECG-QM and the role of H_2O_2 in TMECG-induced downregulation of DHFR. A: Inhibition of superoxide-NBT reduction by TMECG and TMECG-QM. B: H_2O_2 downregulation of DHFR expression. Confluent SK-MEL-28 cells were exposed to H_2O_2 (50 and 100 μM) before Western blot analysis of DHFR expression. A representative Western blot for protein expression and grouped densitometric data $\pm$ SD from eight independent experiments are presented. $^*P < 0.05$ for treated samples when compared with control experiments. C: DHFR expression in SK-MEL-28 cells after 24 h vehicle and TMECG treatments with and without folate-catalase preincubation. A representative Western blot for protein expression and grouped densitometric data $\pm$ SD from eight independent experiments is presented.

Figure 5C shows that the addition of folate-catalase (200 units/ml) reversed the TMECG-induced downregulation of DHFR. These data indicate the importance of intracellular H_2O_2 production in the action of TMECG on DHFR expression in melanoma cells.

DISCUSSION

Some catechins inhibit cancer cell proliferation [Jung and Ellis, 2001]. Because of the therapeutic problems associated with their poor stability and low cellular uptake, we synthesized a methylated derivative of ECG (TMECG), which we observed to be more efficient against melanoma cells. The signaling event cascade that results from treating melanoma with TMECG is illustrated in Figure 6. TMECG is effectively transported to melanoma cells and the melanosome by passive diffusion, where it is activated by the melanosome enzyme tyrosinase to form a quinone methide intermediate with an open structure (TMECG-QM) [Sánchez-del-

Campo et al., 2009a]. After transport to the cytosol, this compound inhibits DHFR and depletes THF coenzymes yielding a subsequent accumulation of DHF. DHF has been shown to be a good inhibitor of MTHFR [Lucock and Roach, 2005], enhancing the potency of the antifolate compounds. Here, we show that DHF also inhibits QDPR in a non-competitive manner, which results in H_4B deficiency and the uncoupling of eNOS. Although it has been proposed that DHFR catalyzes the regeneration of H_4B in several cell types [Chalupsky and Cai, 2005; Sugiyama et al., 2009], the inhibition of QDPR by DHF could explain the oxidative inactivation of H_4B in melanoma cells treated with TMECG. Therefore, the involvement of DHFR in this step remains to be determined. In any case, uncoupling eNOS results in high superoxide production. Direct depletion of H_4B by reaction with TMECG-QM is not a possibility because this oxidized compound was very stable in the presence of H_4B. However, we demonstrated that TMECG-QM is an efficient scavenger of superoxide and that superoxide is quickly transformed in the presence of this compound into H_2O_2, which has been implicated in the downregulation of several genes, including DHFR and QDPR [Hasse
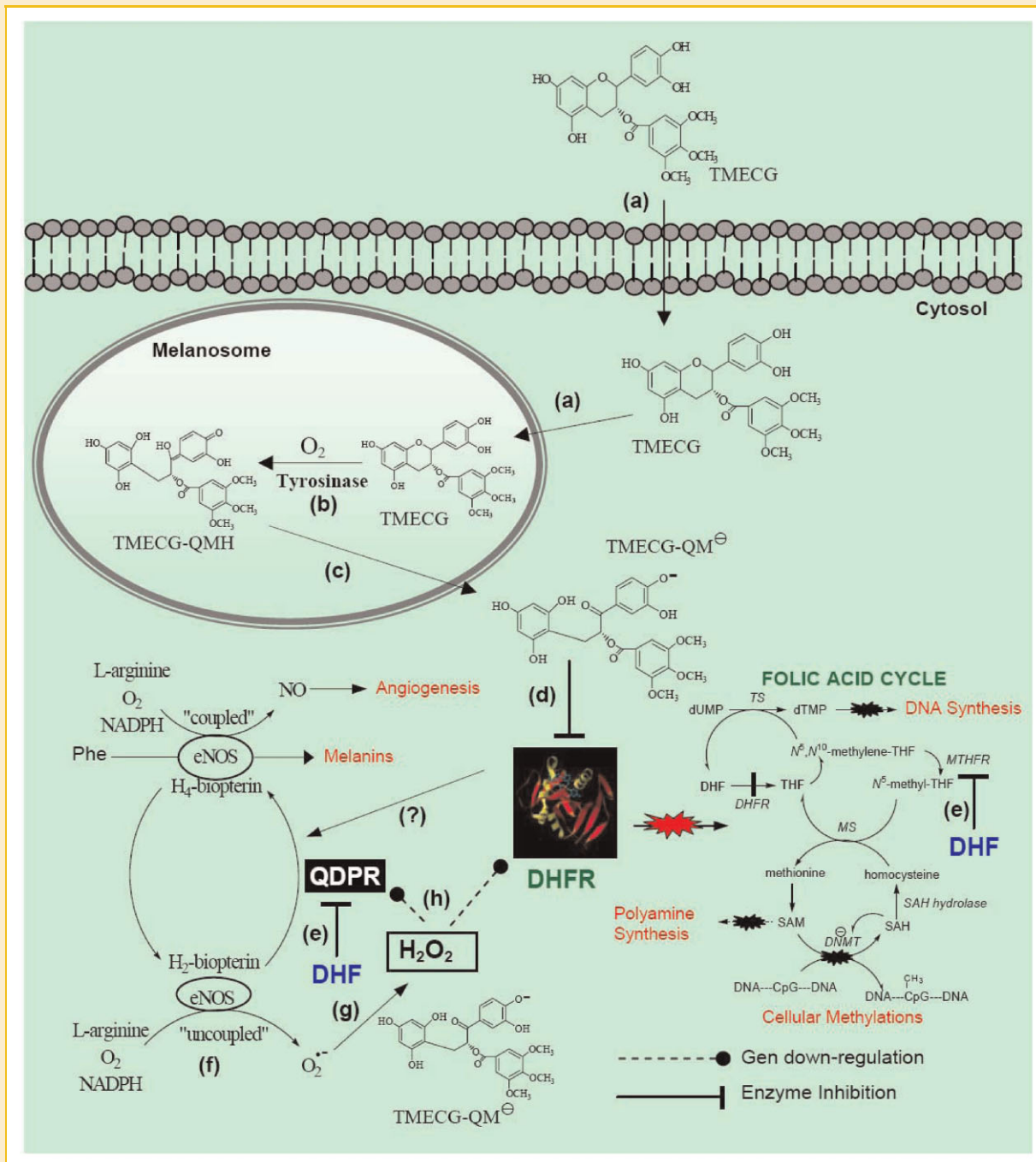
Fig. 6. Schematic mechanism underlying TMECG downregulation of DHFR. After plasmatic and melanosome membrane transport (a), TMECG is specifically activated by tyrosinase (b). Because of the low pH of this organelle, TMECG–QM is predominantly in its neutral charged form, which would leave the melanosome and enter the cytosol due to its high stability and the absence of formal charge (c). The slightly basic pH of the cytosol makes the anionic form of TMECG–QM predominant; it is trapped in this compartment due to its formal negative charge. Its concentration increases in this cellular compartment, where it binds to DHFR (d). As a consequence of DHFR inhibition, intracellular levels of THF coenzymes decrease, resulting in an increase in DHF, which inhibits MTHFR and QDPR enzymes (e). As a consequence of QDPR inhibition, there is an imbalance of biopterin coenzymes, resulting in eNOS reaction uncoupling and the production of excess superoxide (f). Superoxide is efficiently scavenged by TMECG–QM with subsequent H_2O_2 increase (g). Excess H_2O_2 downregulates QDPR and DHFR expression (h). [Color figure can be viewed in the online issue, which is available at www.interscience.wiley.com.]

et al., 2004; Chalupsky and Cai, 2005]. Additionally, H_2O_2 could also inhibit the QDPR reaction, as has been proposed to occur in vitiligo, where excessive H_2O_2 production deactivates QDPR by interacting with Met-146 and Met-151 in the NADH binding site of the enzyme [Hasse et al., 2004]. Taken together, the results strongly suggest that TMECG, or more specifically TMECG-QM, has a dual action on melanoma cells. First, it acts as an antifolate compound, disturbing folic acid metabolism, inhibiting H_4B recycling and inducing

superoxide production. Second, it acts as an efficient antioxidant scavenger of superoxide anions. It is this duality that may be of importance for its action. Classical antifolate compounds are very effective in inhibiting DHFR but the lack of an antioxidant property may be the cause of the lack of DHFR downregulation. In cells treated with antifolates, the common effect is the overexpression of DHFR, which may be responsible for cell resistance to antifolates and is probably the reason that these compounds fail to treat melanoma [Zhao and Goldman, 2003]. In addition, antioxidant therapies have little effect on melanoma. It is interesting to speculate that unsatisfactory outcomes of some of these antioxidant therapies are partially due to their ineffectiveness in uncoupling the eNOS reaction [Chalupsky and Cai, 2005].

Although this study concentrates on explaining the mechanism by which TMECG downregulates DHFR, it is easy to deduce the strong consequences associated with such downregulation. In general, for cancer cells, disrupted folic acid metabolism inhibits DNA and RNA synthesis, alters DNA methylation, and modulates multiple signaling pathways for survival and cellular death [Schweitzer et al., 1990]. For melanoma cells in particular, the disruption of folic acid metabolism and its revealed connection with the recycling of H_4B may also have additional importance. H_4B is the cofactor for phenylalanine and tyrosine hydroxylases, which supply tyrosine and L-dopa for melanin biosynthesis. Inhibition of this pathway has been proven to be a reasonable therapy for melanoma, indicating the importance of this pathway in melanoma survival [Riley, 2003]. In addition to melanin pathway disruption, the observed inhibition of NO production and the uncoupling of eNOS activity by TMECG treatment may also have additional consequences for melanoma cell apoptosis, angiogenesis, and metastasis. Although the role of NO in the regulation of apoptosis is controversial [Choi et al., 2002], recent studies indicated that NO may protect cells from apoptosis induced by multiple stimuli, such as TNFα, Fas, the removal of growth factors or UV irradiation [Choi et al., 2002]. The antiapoptotic effect of NO can be achieved through regulating the expression of apoptosis-protective genes such as heat shock protein 70 and Bcl-2, inhibiting Bcl-2 cleavage, cytochrome *c* release, and ceramide formation, and directly inhibiting caspase-3 and caspase-8 by *S*-nitrosylation [Tong and Li, 2004]. Moreover, eNOS and associated NO can promote angiogenesis, tumor cell proliferation, mobility and invasiveness [Ying and Hofseth, 2007]. Disrupting eNOS expression inhibits the metastatic ability of non-immunogenic B16 melanoma cells in syngenic mice and tumor-induced expression of host eNOS enhances melanoma metastasis and pleural effusion, at least in part through the regulation of vascular formation and vessel permeability [Srivastava et al., 2003]. The absence of eNOS expression has been correlated with decreased VEGF expression and tumor angiogenesis [Wang et al., 2001]. The implication of eNOS in the metastatic and angiogenic events of melanoma, together with the depletion of its essential coenzyme, H_4B, in the presence of TMECG, could explain the effectiveness observed in experiments with mouse melanoma models [Sánchez-del-Campo et al., 2009a]. Thus, targeting eNOS may be a viable strategy for cancer prevention and treatment [Ying and Hofseth, 2007]. Here, we demonstrate that co-targeting the folic acid pathway, the H_4B recycling step and the eNOS reaction in melanoma could be a promising therapy for this fatal skin pathology.

ACKNOWLEDGMENTS

REFERENCES

Benov L. 2001. How superoxide radical damages the cell. Protoplasma 217:33–36.

Bevers LM, Braam B, Post JA, van Zonneveld AJ, Rabelink TJ, Koomans HA, Verhaar MC, Joles JA. 2006. Tetrahydrobiopterin, but not L-arginine, decreases NO synthase uncoupling in cells expressing high levels of endothelial NO synthase. Hypertension 47:87–94.

Cai H. 2005. NAD(P)H oxidase-dependent self-propagation of hydrogen peroxide and vascular disease. Circ Res 96:818–822.

Cai H, Griendling KK, Harrison DG. 2003. The vascular NAD(P)H oxidases as therapeutic targets in cardiovascular diseases. Trends Pharmacol Sci 24:471–478.

Chalupsky K, Cai H. 2005. Endothelial dihydrofolate reductase: Critical for nitric oxide bioavailability and role in angiotensin II uncoupling of endothelial nitric oxide synthase. Proc Natl Acad Sci USA 102:9056–9061.

Choi BM, Pae HO, Jang SI, Kim YM, Chung HT. 2002. Nitric oxide as a proapoptotic as well as anti-apoptotic modulator. J Biochem Mol Biol 35:116–126.

Firgaira FA, Cotton RG, Danks DM. 1981. Isolation and characterization of dihydropteridine reductase from human liver. Biochem J 197:31–43.

Garcia-Molina F, Muñoz JL, Varon R, Rodriguez-Lopez JN, Garcia-Canovas F, Tudela J. 2007. Effect of tetrahydropteridines on the monophenolase and diphenolase activities of tyrosinase. J Enzyme Inhib Med Chem 22:383–394.

Halliwell B. 1978. Superoxide-dependent formation of hydroxyl radicals in the presence of iron chelates: Is it a mechanism for hydroxyl radical production in biochemical systems? FEBS Lett 92:321–326.

Hasse S, Gibbons NC, Rokos H, Marles LK, Schallreuter KU. 2004. Perturbed 6-tetrahydrobiopterin recycling via decreased dihydropteridine reductase in vitiligo: More evidence for H_2O_2 stress. J Invest Dermatol 122:307–313.

Jung YD, Ellis LM. 2001. Inhibition of tumour invasion and angiogenesis by epigallocatechin-gallate (EGCG), a major component of green tea. Int J Exp Path 82:309–316.

Kojima H, Sakurai K, Kikuchi K, Kawahara S, Kirino Y, Nagoshi H, Hirata Y, Nagano T. 1998. Development of a fluorescent indicator for nitric oxide based on the fluorescein chromophore. Chem Pharm Bull 46:373–375.

Lee S, Murthy N. 2007. Targeted delivery of catalase and superoxide dismutase to macrophages using folate. Biochem Biophys Res Commun 360:275–279.

Lucock MD, Roach PD. 2005. The antifolate activity of tea catechins. Cancer Res 65:8573.

Moat SJ, Doshi SN, Lang D, McDowell IF, Lewis MJ, Goodfellow J. 2004. Treatment of coronary heart disease with folic acid: Is there a future? Am J Physiol Heart Circ Physiol 287:H1–H7.

Nano R, Invernizzi R, Facoetti A, Raimondi E, Moralli D, Gerzeli G. 2003. Quantification of the DHFR gene in blast cells of leukaemia patients by fluorescence in situ hybridisation. Anticancer Res 23:3883–3887.

Navarro-Peran E, Cabezas-Herrera J, Garcia-Canovas F, Durrant MC, Thorneley RN, Rodriguez-Lopez JN. 2005. The antifolate activity of tea catechins. Cancer Res 65:2059–2064.

Navarro-Peran E, Cabezas-Herrera J, Sánchez-del-Campo LS, Rodriguez-Lopez JN. 2007. Effects of folate cycle disruption by the green tea polyphenol epigallocatechin-3-gallate. Int J Biochem Cell Biol 39:2215–2225.

Riley PA. 2003. Melanogenesis and melanoma. Pigment Cell Res 16:548–552.

Sánchez-del-Campo LS, Rodríguez-López JN. 2008. Targeting the methionine cycle for melanoma therapy with 3-O-(3,4,5-trimethoxybenzoyl)-(-)-epicatechin. Int J Cancer 123:2446–2455.

Sánchez-del-Campo L, Otón F, Tárraga A, Cabezas-Herrera J, Chazarra S, Rodríguez-López JN. 2008. Synthesis and biological activity of a 3,4,5-trimethoxybenzoyl ester analogue of epicatechin-3-gallate. J Med Chem 51:2018–2026.

Sánchez-del-Campo L, Tárraga A, Montenegro MF, Cabezas-Herrera J, Rodríguez-López JN. 2009a. Melanoma activation of 3-O-(3,4,5-trimethoxybenzoyl)-(-)-epicatechin to a potent irreversible inhibitor of dihydrofolate reductase. Mol Pharm 6:883–894.

Sánchez-del-Campo L, Montenegro MF, Cabezas-Herrera J, Rodríguez-López JN. 2009b. The critical role of alpha-folate receptor in the resistance of melanoma to methotrexate. Pigment Cell Melanoma Res 22:588–600.

Schweitzer BI, Dicker AP, Bertino JR. 1990. Dihydrofolate reductase as a therapeutic target. FASEB J 4:2441–2452.

Sowers R, Toguchida J, Qin J, Meyers PA, Healey JH, Huvos A, Banerjee D, Bertino JR, Gorlick R. 2003. mRNA expression levels of E2F transcription factors correlate with dihydrofolate reductase, reduced folate carrier, and thymidylate synthase mRNA expression in osteosarcoma. Mol Cancer Ther 2:535–541.

Spitz DR, Oberley LW. 1989. An assay for superoxide dismutase activity in mammalian tissue homogenates. Anal Biochem 179:8–18.

Srivastava A, Ralhan R, Kaur J. 2003. Angiogenesis in cutaneous melanoma: Pathogenesis and clinical implications. Microsc Res Tech 60:208–224.

Sugiyama T, Levy BD, Michel T. 2009. Tetrahydrobiopterin recycling: A key determinant of eNOS-dependent signaling pathways in cultured vascular endothelial cells. J Biol Chem 284:12691–12700.

Thony B, Auerbach G, Blau N. 2000. Tetrahydrobiopterin biosynthesis, regeneration and functions. Biochem J 347:1–16.

Tong X, Li H. 2004. eNOS protects prostate cancer cells from TRAIL-induced apoptosis. Cancer Lett 210:63–71.

Tu YT, Tao J, Liu YQ, Li Y, Huang CZ, Zhang XB, Lin Y. 2006. Expression of endothelial nitric oxide synthase and vascular endothelial growth factor in human malignant melanoma and their relation to angiogenesis. Clin Exp Dermatol 31:413–418.

Vasquez-Vivar J, Whitsett J, Martasek P, Hogg N, Kalyanaraman B. 2001. Reaction of tetrahydrobiopterin with superoxide: EPR-kinetic analysis and characterization of the pteridine radical. Free Radic Biol Med 31:975–985.

Wang B, Xiong Q, Shi Q, Tan D, Le X, Xie K. 2001. Genetic disruption of host nitric oxide synthase II gene impairs melanoma-induced angiogenesis and suppresses pleural effusion. Int J Cancer 91:607–611.

Werner-Felmayer G, Golderer G, Werner ER. 2002. Tetrahydrobiopterin biosynthesis, utilization and pharmacological effects. Curr Drug Metab 3:159–173.

Ying L, Hofseth LJ. 2007. An emerging role for endothelial nitric oxide synthase in chronic inflammation and cancer. Cancer Res 67:1407–1410.

Zhao R, Goldman ID. 2003. Resistance to antifolates. Oncogene 22:7431–7457.